ADVANCED FUNCTIONAL MATERIALS
www.afm-journal.de

MOF Nano-Vesicles and Toroids: Self-Assembled Porous Soft-Hybrids for Light Harvesting

Venkata M. Suresh, Subi J. George, and Tapas Kumar Maji**

Metal-organic vesicular and toroid nanostructures of Zn(OPE)·2H$_2$O are achieved by coordination-directed self-assembly of *oligo*-phenyleneethynylene-dicarboxylic acid (OPEA) as a linker with Zn(OAc)$_2$ by controlling the reaction parameters. Self-assembled nanostructures are characterized by powder X-ray diffraction, field emission scanning electron microscopy (FESEM), transmission electron microscopy (TEM), and adsorption study. The amphiphilic nature of the coordination-polymer with long alkyl chains renders different soft vesicular and toroidal nanostructures. The permanent porosity of the framework is established by gas adsorption study. Highly luminescent 3D porous framework is exploited for Froster's resonance energy transfer (FRET) by encapsulation of a suitable cationic dye (DSMP) which shows efficient funneling of excitation energy. These results demonstrate the dynamic and soft nature of the MOF, resulting in unprecedented vesicular and toroidal nanostructures with efficient light harvesting applications.

1. Introduction

Metal-organic frameworks (MOFs), an interesting class of inorganic–organic hybrid porous materials,[1] showed promising applications in different fields including gas storage, separation, catalysis, sensors, and drug delivery.[2] Multi-functional luminescent MOFs with a chromophoric linker combined with permanent porosity are gaining attention,[3] and are attractive candidates for optoelectronics too.[4] However, the solution processability of these hybrid frameworks is one of the critical features to be addressed for the advancement of this field. In this context, nanoscale MOFs (NMOFs), are an exciting class of tunable and modular soft-hybrids with unprecedented processable nature.[5] These soft luminescent porous hybrids would show guest dependent emission either via energy-transfer or through the formation of intermolecular complexes such as excimer or exciplex and, hence, are striking materials for sensor or energy-transfer applications.[6] Recently, light-harvesting organic-inorganic hybrids have gathered immense attention as transparent luminescent materials.[7] Although, various organic assemblies have been well-studied for light-harvesting applications,[8] they often exhibit fluorescence quenching due to intermolecular interactions, either in the self-assembled state or on solid-substrates. In this context, the nanoscale periodicity of the inorganic components in the hybrid design would help the spatial organization of organic donor and acceptor chromophores, thereby minimizing the inter-chromophoric interactions to enhance the luminescence quantum yield. With this objective, several elegant designs based on zeolites,[9] mesoporous organosilica (PMO),[10] and clay composites[11] have been reported as efficient light-harvesting hybrids. We envision that the design of supramolecular MOF framework with fluorescent organic linkers will result in luminescent inorganic-organic soft-hybrids with the dynamic feature of being able to change their structure according to the external stimuli. The dynamic nature of the framework would provide a pathway for modulating their nanostructure morphology and for the guest encapsulation.[12] Moreover, these self-assembled soft-hybrids would act as efficient light-harvesting scaffolds for non-covalently entrapped dye molecules and would have processable features for luminescent device applications. With this objective, we have designed the coordination-assisted self-assembly of *oligo*-phenyleneethynylenedicarboxylic acid (OPEA), with solubilizing side chains. Although OPE derivatives are well studied from organic assembly point of view for optoelectronic functions,[13] their coordination-assisted self-assembly has not yet been studied. Crystalline NMOFs of different morphologies like sphere, cube, rod, hollow sphere have been reported.[14] However, the nano-architectures with vesicular or toroidal morphologies are yet to be realized in metal-organic framework systems. Here, we report unprecedented MOF nanostructures, such as vesicles and toroids, achieved by the coordination-assisted self-assembly of OPEA with Zn^{II} metal ion. We also demonstrate that these porous soft-hybrids can funnel the excitation energy to appropriate acceptor molecule, and hence acts as an efficient light-harvesting antenna.

2. Results and Discussion

The coordination polymer is prepared by mixing Zn(OAc)$_2$·2H$_2$O (1 mM) and OPEA (1 mM) in tetrahydrofuran

V. M. Suresh, Prof. T. K. Maji
Chemistry and Physics of Materials Unit
Jawaharlal Nehru Centre for Advanced
Scientific Research
Jakkur, Bangalore 560064, India
E-mail: tmaji@jncasr.ac.in
Dr. S. J. George, Prof. T. K. Maji
New Chemistry Unit
Jawaharlal Nehru Centre for Advanced Scientific Research
Jakkur, Bangalore 560064, India
E-mail: george@jncasr.ac.in

DOI: 10.1002/adfm.201301178

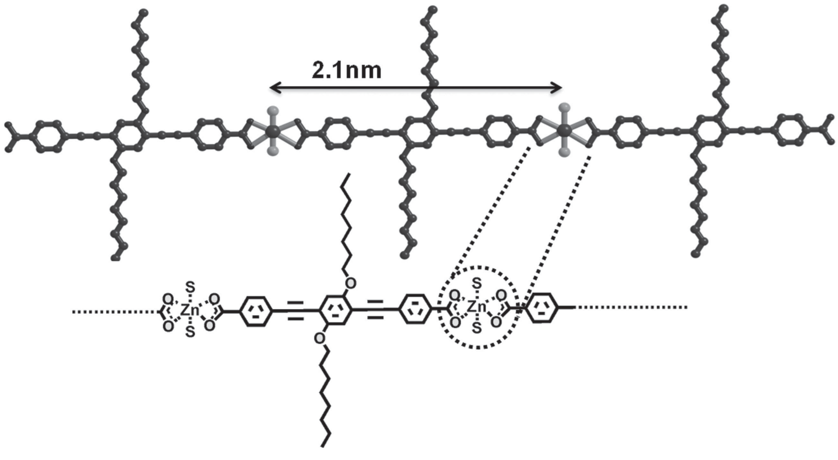

Scheme 1. Self-assembled 1D coordination chain of Zn(OPE)·$(H_2O)_2$, below: showing the coordination environment around Zn(II) and the chromophoric linker OPE.

(THF) (5 mL) solution at room temperature. Coordination of Zn^{II} ions to the carboxylate groups of the ligand is evident from the instantaneous formation of white colloids. The reaction is further continued for 6 h to yield a neutral coordination polymer with a molecular formula of Zn(OPE)·$2H_2O$ (**1**), calculated through elemental analysis, in which the OPE and metal ions are assembled in a 1:1 alternate fashion (**Scheme 1**). The presence of the metal ions in the coordination polymer is further confirmed by energy dispersive X-ray analysis (EDAX) (Figure S1, Supporting Information). Fourier transform IR spectroscopy (FTIR) shows strong peaks at 1602 cm^{-1} and 1411 cm^{-1}, characteristic of the carboxylate stretching frequency (Figure S2a, Supporting Information), and $\Delta \approx 191$ cm^{-1} suggesting the bidentate coordination of the Zn^{II} metal ions, as shown in Scheme 1. Interestingly, gas adsorption studies of **1** provided insights into the three-dimensional (3D) self-organization of the coordination polymer **1** into a supramolecular porous framework structure. Thermogravimetric analysis (TGA) of **1** (Figure S2b, Supporting Information) shows an initial weight loss of 3.3% at 110 °C corresponding to the loss of coordinated water molecules, and the resulting desolvated framework is stable up to 350 °C. Hence, compound **1** was desolvated at 110 °C, before performing the adsorption measurements of N_2 (at 77 K) and CO_2 (at 195 K). Gas adsorption of the N_2 (kinetic diameter = 3.64 Å) at 77 K shows a typical type II profile (**Figure 1**a) and the pore size distribution (NLDFT method) suggests the presence of both micro and mesopores (Figure S3, Supporting Information). Furthermore, CO_2 adsorption measurement of **1** shows a sharp uptake of CO_2 at low pressure regions, with a typical type I profile, unveiling the microporous nature of the framework (Figure 1b). The amount of the CO_2 uptake at the end point is found to be 48.6 mL g^{-1} suggesting 1.34 CO_2 molecules per formula unit, and the corresponding Langmuir surface area is calculated to be 273 m^2 g^{-1}. Powder X-ray diffraction (PXRD) measurements of **1** provided structural insights into the self-assembled framework. The PXRD pattern (Figure 1c) of **1** shows several peaks corresponding to the d-spacings of 21.01 Å, 12.52 Å, and 4 Å. The intense low angle peak with a d-spacing of 21 Å is in agreement with the repeating distance between the two metal centers in the 1D coordination polymer chains (Scheme 1). The stacking of these 1D polymeric chains through π–π interactions is further evident from the presence of a diffraction peak with d-spacing value of 4 Å. We envisage that the presence of hydrophobic interactions arising from the alkyl chains leads to the three-dimensionally extended supramolecular framework, in which the π-stacked planes of the coordination polymer chains are connected via interdigitated alkyl chains. This is supported by the presence of the peak at 7.73° corresponding to a d-spacing value of 1.2 nm, suggesting that alkyl chains are indeed interdigitated. A proposed model of this supramolecular framework structure is schematically shown in Figure 1d. Interestingly, the micropore dimensions calculated from the adsorption measurements (≈13 Å) are in agreement with the proposed interdigitated 3D structure. The mesoporosity observed in the N_2 adsorption measurements can be attributed to the interparticle separation. The self-assembled structure of **1** was further investigated using various microscopic techniques (field emission scanning electron microscope (FESEM) and transmission electron microscope (TEM)). FESEM and TEM analyses of **1** showed clusters of small flaky particles having dimensions of 0.8–2 µm (Figure 1e and Figure S4, Supporting Information). Interestingly, high-resolution TEM analysis at the edges of this particle showed a highly ordered structure, as evident from the regularly spaced dark lines with an interspacing distance of 0.8–1.1 nm (Figure 1f,g and Figure S4, Supporting Information). The close agreement between the periodic spacing with that of the PXRD data suggests that the dark lines correspond to the π-stacked polymer chains, whereas the bright regions are filled with interdigitated alkyl chains of successive 2D sheets. We envisage that 1D coordination chains would exhibit an amphiphilic nature because of the presence of nonpolar flexible side chains and polar carboxylate groups attached to Zn^{II} atoms. It is well known that the morphology of amphiphilic molecules can be controlled with structural modifications and thereby changing the polar–nonpolar ratio.[15] This provides an opportunity to modulate the nanostructure morphology of these hybrid assemblies in polar solvents by varying the reaction parameters, which would result in coordination-polymeric chains with different lengths. Furthermore, the noncovalent nature of the present framework would render dynamic nature to these hybrid assemblies to facilitate structural re-organization. In order to validate this proposal, we have varied the reaction time from 6 h to 24 h and analyzed the morphology at periodic intervals. Remarkably, hybrid flaky-nanoparticles transformed into spherical vesicular structures of 100–300 nm diameter upon continuing the reaction for 24 h, as evident from the FESEM analyses (**Figures 2**a,b). The formation of nanovesicles is further evident from the TEM analysis, which clearly showed the presence of spherical assemblies with dark shell and bright core (Figures 2c). Since the alkyl regions of these hybrid assemblies are more soluble in the reaction solvent THF, we believe that these nanostructures are inverse vesicles with alkyl chains

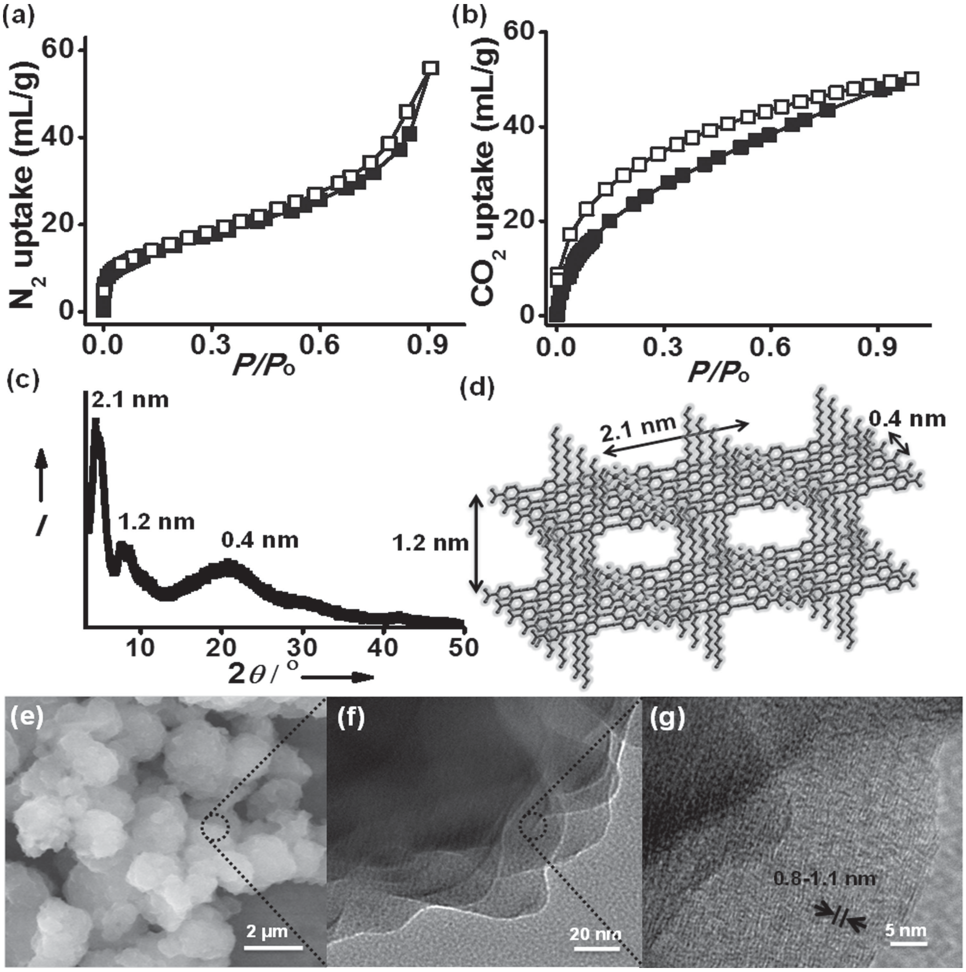

Figure 1. a) N$_2$ (at 77 K) and b) CO$_2$ (at 195 K) adsorption isotherms for desolvated compound **1**. c) PXRD pattern of **1**. d) Schematic representation of the 3D supramolecular organization of **1** proposed based on the PXRD data. e) FESEM image of **1** after 6 h reaction time showing the clusters of flaky particles. f) TEM image of a spherical particle. g) High resolution TEM image of **1** showing structural ordering of 1D coordination chains to a higher dimensional supramolecular organization through the interdigitation of alkyl chains.

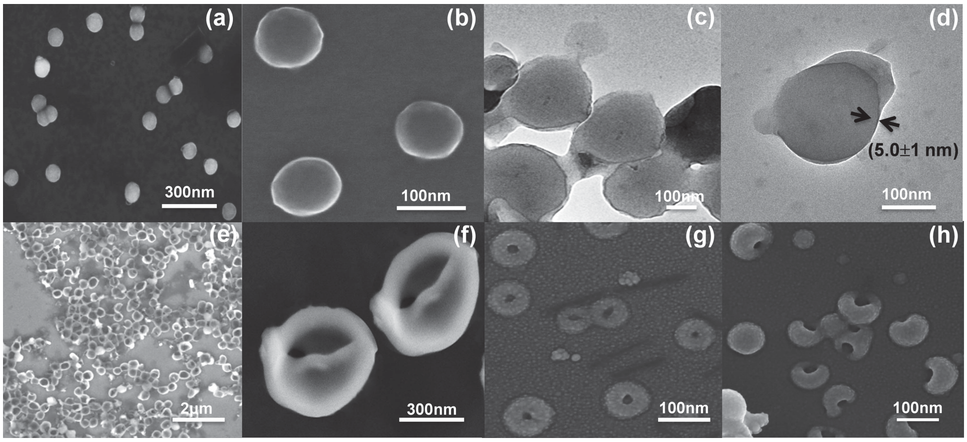

Figure 2. MOF nanostructures. a,b) FESEM images of nanovesicles of **1**. c) TEM images of nanovesicles. d) TEM of nanovesicles at higher magnification showing light core and thick shell of thickness 5.0 ± 1 nm. FESEM images of e) nanobowls, f) open nanobowls, g) toroids, and h) hemispherical shapes.

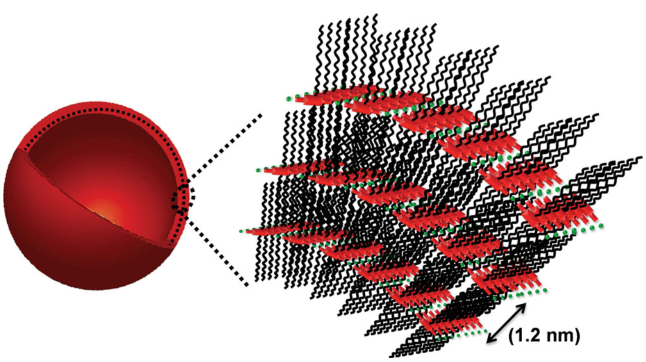

Figure 3. Schematic illustration of the proposed molecular organization of **1** in multilayered inverse vesicles.

projected to the exterior, as shown in the schematic representation (**Figure 3**). Detailed TEM analysis revealed a thickness of 5 ± 1 nm for the dark regions, which suggests that vesicular walls consists of 5 to 6 interdigitated layers of π-stacked polymeric chains (Figure 2d). In this context, thin films of layered MOF nanostructures have been recently documented for selective permeability and gas sensing applications.[16] Interestingly, further reaction up to 32–34 h resulted in bowl, toroidal, and hemispherical shaped nanostructures of 100–300 nm in diameter, as evident from the FESEM (Figures 2e–h), TEM, and AFM images (Figure S5, Supporting Information). PXRD analyses showed that these nanostructures retains the same framework structure of the initial flaky particles (Figure S6, Supporting Information), suggesting that changes in the length (degree of polymerization) and amphiphilic nature of coordination polymer chains drive the formation of these unprecedented hybrid nanostructures. To our knowledge, this is the first report of MOF nanovesicles (or toroids).

Flaky nanostructures of **1**, obtained after 6 h exhibit green fluorescence with a maximum at 462 nm upon excitation at 412 nm (Figure S7, Supporting Information). The permanent porosity and intense luminescence behavior of **1** prompted us to explore the Förster resonance energy transfer (FRET) from OPE linkers to non-covalently encapsulated acceptor dye molecules. In the present study, we have chosen the cationic dye, *trans*-4-[4-(dimethylamino)styryl]-1-methylpyridinium iodide (DSMP) as the excitation energy acceptor (λ_{max} = 480 nm, λ_{em} = 615 nm), because of the good spectral overlap between its absorption with the emission of **1** (**Figure 4**a). Room temperature mixing of the DSMP (2 mol%) with activated compound **1** in dry THF for 24 h resulted in the formation of a stable, mixed nanocolloids, Zn(OPE)–DSMP (**2**). The mixed hybrids were separated by centrifugation and dried under vacuum at room temperature. Similar PXRD patterns of **2** with that of **1** reveal that there are no structural changes in the framework upon guest encapsulation of the dye molecules (Figure S8, Supporting Information). The inclusion of DSMP into the coordination network is further confirmed by ^{1}H NMR (Figure S9, Supporting Information). ^{1}H NMR of **2** by disintegrating in DCl shows the presence of 0.04 DSMP molecules per formula unit of the framework. Furthermore, the TGA analysis of the **2** displays an additional step at 310 °C suggesting the presence of DSMP in the framework (Figure S10, Supporting Information). We believe that cationic DSMP dyes are located in the relatively polar regions of the MOF created by the carboxylate groups of OPEA, chelating the zinc metal ion in the coordination chain (Scheme 1). When the dye loaded mixed hybrids, **2** is selectively excited at 412 nm, the framework emission at 462 nm is completely quenched, whereas a strong DSMP emission is appeared at 625 nm. This indicates an efficient excitation energy transfer from the framework to the encapsulated dye molecules (Figure 4b). This resonance energy transfer is further supported by the excitation spectrum of **2** collected at the DSMP emission (625 nm), which showed a maximum at 425 nm clearly suggesting the contribution of OPE linkers to the observed emission (Figure S11, Supporting Information). In addition, the direct excitation of DSMP molecules in **2** at 480 nm shows less intensity compared to the indirect excitation at 412 nm, clearly indicating a light-harvesting process through FRET mechanism. Fluorescence decay profiles of the framework loaded with 0.5 mol% of DSMP monitored at the OPE emission (462 nm) showed shortening (2.3 ns) of life-time compared to that of pure framework **1** (5.9 ns), providing further proof for energy transfer. In addition,

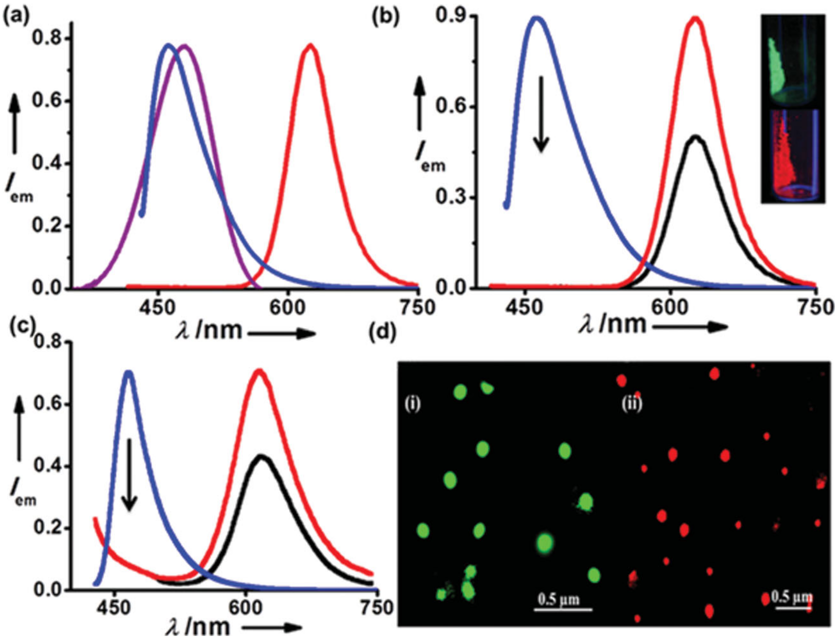

Figure 4. a) Normalized absorption (violet) and emission spectra (red) of DSMP in solution and emission spectra of **1** (blue) in solid state. b) Normalized emission spectra of **1** excited at 412 nm (blue), Zn(OPE)–DSMP (**2**) excited at 412 nm (red) and at 480 nm (black, indirect excitation); inset: images of **1** (green) and **2** (red) under UV-lamp. c) Normalized emission spectra of nanovesicles of **1** (blue), and DSMP included nanovesicles excited at 412 nm (red) and 480 nm (black). Confocal microscopy images of d) (i) nanovesicles of **1**, and (ii) DSMP incorporated nanovesicles of **2**.

life time of DSMP encapsulated in **2** monitored at 625 nm is longer (5.1 ns) than free DSMP molecules (2.9 ns) (Figure S12, Supporting Information). Motivated by these observations, we further extended energy transfer studies to the vesicular hybrid nanostructures of **1** by loading DSMP dye (2 mol%). Fluorescence measurements of these mixed hybrid vesicles have also shown a very efficient energy transfer as shown in Figure 4c. This is further evident form confocal fluorescence microscopic images of the hybrid vesicles (Figure 4d) which showed green and red emission, respectively.

3. Conclusions

The results presented here illustrate a novel strategy to prepare unprecedented nanoscale MOF morphologies like vesicles, toroids, and bowls by controlling the coordination interactions between metal (Zn^{II}) and linker (OPEA) during the self-assembly process. The inherent porous nature of the MOF system with soft modular nanoscale morphologies would enhance dynamicity for guest uptake. The porosity of these MOF nanostructures has been further exploited for the spatial organization of acceptor molecules, which resulted in an efficient excitation energy transfer from the luminescent framework to the dye molecules in their pores. The functionalities of porous metal-organic vesicular structures can be extended as a low density capsule for controlled release of drugs or dyes, and as a microreactor for catalysis.

4. Experimental Section

Synthesis of Zn(OPE)·2H$_2$O: $Zn(OAc)_2\cdot 2H_2O$ (1eq) were dissolved in 5 mL THF and then drop-wise added to a THF solution of OPE (1eq) under continuous stirring. The white colloids started forming within few minutes, continuing for further 6 h at room temperature. These white colloids were centrifuged, thoroughly washed with THF, and dried under vacuum for 6 h. Similar reactions have been performed for different time scale like 24, 32, 36, and 42 h. The resultant products were characterized by different techniques. Yield: 54%. Elemental analysis for $ZnC_{40}H_{48}O_8$. Calculated: C, 66.5; H, 6.69. Found: C, 64.4; H, 6.7. FTIR in KBr (cm^{-1}): 3441(br), 2925(sh), 2854(sh), 2208(w), 1602(vs), 1531(w), 1411(vs), 1280(w), 1216(sh), 1162(s), 1018(br), 862(w), 781(s).

Preparation of Zn(OPE)-DSMP: The desolvated ZnOPE (10 mg) was taken in 3 mL of dry THF and then DSMP dye (2 mol%) was added. The reaction mixture was stirred for 24 h at room temperature. It was centrifuged and washed with dichloromethane (DCM), THF several times and dried under vacuum at room temperature. The product was characterized by the several techniques.

Supporting Information

Supporting Information is available from the Wiley Online Library or from the author.

Acknowledgements

The authors thank Prof. C. N. R. Rao for his support and encouragement, Prof. G. U. Kulkarni for Veeco Lab facilities. The authors acknowledge Selvi (FESEM) and Usha (TEM) for microscopic measurements. M.V.S. thanks CSIR (Govt. of India) for fellowship. T.K.M. gratefully acknowledges Sheikh Saqr fellowship.

Received: April 6, 2013
Revised: April 25, 2013

---

[1] a) S. Kitagawa, R. Kitaura, S. Noro, *Angew. Chem. Int. Ed.* **2004**, *43*, 2334; b) S. L. James, *Chem. Soc. Rev.* **2003**, *32*, 276; c) G. Ferey, *Dalton Trans.* **2009**, 4400; d) J. J. I. V. Perry, J. A. Perman, M. J. Zaworotko, *Chem. Soc. Rev.* **2009**, *38*, 1400; e) H.-L. Jiang, Q. Xu, *Chem. Commun.* **2011**, *47*, 3351; f) S. T. Meek, J. A. Greathouse, M. D. Allendorf, *Adv. Mater.* **2011**, *23*, 249; g) C. Janiak, *Dalton Trans.* **2003**, 2781; h) C. N. Rao, S. Natarajan, R. Vaidhyanathan, *Angew. Chem. Int. Ed.* **2004**, *43*, 1466; i) T. K. Maji, S. Kitagawa, *Pure Appl. Chem.* **2007**, *79*, 2155; j) O. M. Yaghi, M. O'Keeffe, N. W. Ockwig, H. K. Chae, M. Eddaoudi, J. Kim, *Nature* **2003**, *423*, 705.

[2] a) N. L. Rosi, J. Eckert, M. Eddaoudi, D. T. Vodak, J. Kim, M. O'Keeffe, O. M. Yaghi, *Science* **2003**, *300*, 1127; b) S. Mohapatra, K. P. S. S. Hembram, U. Waghmare, T. K. Maji, *Chem. Mater.* **2009**, *21*, 5406; c) P. Kanoo, A. C. Ghosh, S. T. Cyriac, T. K. Maji, *Chem. Eur. J.* **2012**, *18*, 237; d) N. Nijem, H. Wu, P. Canepa, A. Marti, K. J. J. Balkus, T. Thonhauser, J. Li, Y. J. Chabal, *J. Am. Chem. Soc.* **2012**, *134*, 15201; e) S. Ma, H.-C. Zhou, *Chem. Commun.* **2010**, *46*, 44; f) K. Sumida, D. L. Rogow, J. A. Mason, T. M. McDonald, E. D. Bloch, Z. R. Herm, T.-H. Bae, J. R. Long, *Chem. Rev.* **2012**, *112*, 724; g) J. Lee, O. K. Farha, J. Roberts, K. A. Scheidt, S. T. Nguyen, J. T. Hupp, *Chem. Soc. Rev.* **2009**, *38*, 1450; h) B. Chen, L. Wang, Y. Xiao, F. R. Fronczek, M. Xue, Y. Cui, G. Qian, *Angew. Chem. Int. Ed.* **2009**, *48*, 500; i) P. Horcajada, C. Serre, G. Maurin, N. A. Ramsahye, F. Balas, M. Vallet-Regi, M. Sebban, F. Taulelle, G. Ferey, *J. Am. Chem. Soc.* **2008**, *130*, 6774.

[3] a) C. Y. Lee, O. K. Farha, B. J. Hong, A. A. Sarjeant, S. T. Nguyen, J. T. Hupp, *J. Am. Chem. Soc.* **2011**, *133*, 15858; b) K. Jayaramulu, P. Kanoo, S. J. George, T. K. Maji, *Chem. Commun.* **2010**, *46*, 7906; c) C. A. Bauer, T. V. Timofeeva, T. B. Settersten, B. D. Patterson, V. H. Liu, B. A. Simmons, M. D. Allendorf, *J. Am. Chem. Soc.* **2007**, *129*, 7136; d) K. C. Stylianou, R. Heck, S. Y. Chong, J. Bacsa, J. T. A. Jones, Y. Z. Khimyak, D. Bradshaw, M. J. Rosseinsky, *J. Am. Chem. Soc.* **2010**, *132*, 4119.

[4] a) Y. Takashima, V. Martinez Martinez, S. Furukawa, M. Kondo, S. Shimomura, H. Uehara, M. Nakahama, K. Sugimoto, S. Kitagawa, *Nat. Commun.* **2011**, *2*, 168; b) H. Khajavi, J. Gascon, J. M. Schins, L. D. A. Siebbeles, F. Kapteijn, *J. Phys. Chem. C* **2011**, *115*, 12487; c) W. B. Lin, Z. Y. Wang, L. Ma, *J. Am. Chem. Soc.* **1999**, *121*, 11249; d) O. R. Evans, R. Xiong, Z. Wang, G. K. Wong, W. Lin, *Angew. Chem. Int. Ed.* **1999**, *38*, 536; e) M. Mueller, A. Devaux, C.-H. Yang, L. De Cola, R. A. Fischer, *Photochem. Photobiol. Sci.* **2010**, *9*, 846.

[5] a) J. Della Rocca, D. Liu, W. Lin, *Acc. Chem. Res.* **2011**, *44*, 957; b) A. Carne, C. Carbonell, I. Imaz, D. Maspoch, *Chem. Soc. Rev.* **2011**, *40*, 291; c) B. Liu, O. Shekhah, H. K. Arslan, J. Liu, C. Woell, R. A. Fischer, *Angew. Chem. Int. Ed.* **2012**, *51*, 807; d) W. J. Rieter, K. M. Pott, K. M. L. Taylor, W. Lin, *J. Am. Chem. Soc.* **2008**, *130*, 11584; e) K. Otsubo, T. Haraguchi, O. Sakata, A. Fujiwara, H. Kitagawa, *J. Am. Chem. Soc.* **2012**, *134*, 9605; f) I. Imaz, J. Hernando, D. Ruiz-Molina, D. Maspoch, *Angew. Chem. Int. Ed.* **2009**, *48*, 2325.

[6] a) X. Zhang, M. A. Ballem, M. Ahren, A. Suska, P. Bergman, K. Uvdal, *J. Am. Chem. Soc.* **2010**, *132*, 10391; b) C. A. Kent, D. Liu, L. Ma, J. M. Papanikolas, T. J. Meyer, W. Lin, *J. Am. Chem. Soc.* **2011**, *133*, 12940; c) X. Zhang, M. A. Ballem, Z.-J. Hu, P. Bergman, K. Uvdal, *Angew. Chem. Int. Ed.* **2011**, *50*, 5728; d) H. Xu, F. Liu, Y. Cui, B. Chen, G. Qian, *Chem. Commun.* **2011**, *47*, 3153; e) X. Zhang, Z.-K. Chen, K. P. Loh, *J. Am. Chem. Soc.* **2009**, *131*, 7210.

[7] a) K. V. Rao, K. K. R. Datta, M. Eswaramoorthy, S. J. George, *Chem. Eur. J.* **2012**, *18*, 2184; b) R. Haldar, K. V. Rao, S. J. George, T. K. Maji, *Chem. Eur. J.* **2012**, *18*, 5848.

[8] a) T. Nakashima, N. Kimizuka, *Adv. Mater.* **2002**, *14*, 1113; b) A. Ajayaghosh, S. J. George, V. K. Praveen, *Angew. Chem. Int. Ed.* **2003**, *42*, 332; c) K. Sugiyasu, N. Fujita, S. Shinkai, *Angew. Chem. Int. Ed.* **2004**, *43*, 1229; d) S. J. George, A. Ajayaghosh, P. Jonkheijm, A. Schenning, E. W. Meijer, *Angew. Chem. Int. Ed.* **2004**, *43*, 3422; e) A. Ajayaghosh, V. K. Praveen, C. Vijayakumar, *Chem. Soc. Rev.* **2008**, *37*, 109; f) C. Devadoss, P. Bharathi, J. S. Moore, *J. Am. Chem. Soc.* **1996**, *118*, 9635; g) N. Aratani, D. Kim, A. Osuka, *Acc. Chem. Res.* **2009**, *42*, 1922; h) R. A. Haycock, A. Yartsev, U. Michelsen, V. Sundstrom, C. A. Hunter, *Angew. Chem. Int. Ed.* **2000**, *39*, 3616; i) M. S. Choi, T. Yamazaki, I. Yamazaki, T. Aida, *Angew. Chem. Int. Ed.* **2004**, *43*, 150; j) Y. Ishida, T. Shimada, D. Masui, H. Tachibana, H. Inoue, S. Takagi, *J. Am. Chem. Soc.* **2011**, *133*, 14280.

[9] a) G. Calzaferri, S. Huber, H. Maas, C. Minkowski, *Angew. Chem. Int. Ed.* **2003**, *42*, 3732; b) G. Calzaferri, K. Lutkouskaya, *Photochem. Photobiol. Sci.* **2008**, *7*, 879; c) T. Q. Nguyen, J. Wu, S. H. Tolbert, B. J. Schwartz, *Adv. Mater.* **2001**, *13*, 609.

[10] a) N. Mizoshita, Y. Goto, T. Tani, S. Inagaki, *Adv. Mater.* **2009**, *21*, 4798; b) S. Inagaki, O. Ohtani, Y. Goto, K. Okamoto, M. Ikai, K.-I. Yamanaka, T. Tani, T. Okada, *Angew. Chem. Int. Ed.* **2009**, *48*, 4042; c) T. Q. Nguyen, J. J. Wu, V. Doan, B. J. Schwartz, S. H. Tolbert, *Science* **2000**, *288*, 652; d) Y. Maegawa, N. Mizoshita, T. Tani, S. Inagaki, *J. Mater. Chem.* **2010**, *20*, 4399.

[11] a) K. V. Rao, K. K. R. Datta, M. Eswaramoorthy, S. J. George, *Angew. Chem. Int. Ed.* **2011**, *50*, 1179; b) K. V. Rao, K. K. R. Datta, M. Eswaramoorthy, S. J. George, *Adv. Mater.* **2013**, *25*, 1713.

[12] a) S. Horike, S. Shimomura, S. Kitagawa, *Nat. Chem.* **2009**, *1*, 695; b) S. Shimomura, S. Kitagawa, *J. Mater. Chem.* **2011**, *21*, 5537.

[13] a) K. Becker, P. G. Lagoudakis, G. Gaefke, S. Hoeger, J. M. Lupton, *Angew. Chem. Int. Ed.* **2007**, *46*, 3450; b) P. V. James, P. K. Sudeep, C. H. Suresh, K. G. Thomas, *J. Phys. Chem. A* **2006**, *110*, 4329; c) G. Duvanel, J. Grilj, A. Schuwey, A. Gossauer, E. Vauthey, *Photochem. Photobiol. Sci.* **2007**, *6*, 956.

[14] E. A. Fluegel, A. Ranft, F. Haase, B. V. Lotsch, *J. Mater. Chem.* **2012**, *22*, 10119.

[15] a) M. Masuda, V. Vill, T. Shimizu, *J. Am. Chem. Soc.* **2000**, *122*, 12327; b) R. Iwaura, T. Iizawa, H. Minamikawa, M. Ohnishi-Kameyama, T. Shimizu, *Small* **2010**, *6*, 1131.

[16] a) R. Makiura, S. Motoyama, Y. Umemura, H. Yamanaka, O. Sakata, H. Kitagawa, *Nat. Mater.* **2010**, *9*, 565; b) R. Ameloot, F. Vermoortele, W. Vanhove, M. B. J. Roeffaers, B. F. Sels, D. E. De Vos, *Nat. Chem.* **2011**, *3*, 382.